SCIENCE CHINA PRESS

SCIENCE CHINA Life Sciences
life.scichina.com link.springer.com
https://doi.org/10.1007/s11427-024-2858-5

RESEARCH PAPER

Vibration mechanics involved in buzz pollination lead to size-dependent associations between bumblebees and *Pedicularis* flowers

Yuanqing Xu[1,2], Bentao Wu[3], Mario Vallejo-Marín[4], Peter Bernhardt[5], Mark Jankauski[6], De-Zhu Li[1,7], Stephen Buchmann[8], Jianing Wu[3*] & Hong Wang[1,7*]

[1]Key Laboratory for Plant Diversity and Biogeography of East Asia, Kunming Institute of Botany, Chinese Academy of Sciences, Kunming 650201, China
[2]University of Chinese Academy of Sciences, Beijing 100049, China
[3]School of Advanced Manufacturing, Sun Yat-sen University, Shenzhen 518107, China
[4]Department of Ecology and Genetics, Uppsala University, Uppsala 75236, Sweden
[5]Bayer Herbarium, the Missouri Botanical Garden, Saint Louis 63110, USA
[6]Department of Mechanical and Industrial Engineering, Montana State University, Bozeman 59717, USA
[7]Germplasm Bank of Wild Species & Yunnan Key Laboratory of Crop Wild Relatives Omics, Kunming Institute of Botany, Chinese Academy of Sciences, Kunming 650201, China
[8]Department of Ecology and Evolutionary Biology, and Department of Entomology, University of Arizona, Tucson 85721, USA

*Corresponding authors (Hong Wang, email: wanghong@mail.kib.ac.cn; Jianing Wu, email: wujn27@mail.sysu.edu.cn)

Received 17 October 2024; Accepted 28 January 2025; Published online 12 March 2025

Floral traits modify pollinator behavior and shape the plant-pollinator interaction pattern at ecological and evolutionary levels. Biomechanical traits are important in mediating interactions between flowers and their pollinators in some cases, such as in buzz pollination. During buzz pollination, a bee produces vibrations using its thoracic muscles and transfers these vibrations primarily through its mandibles as it bites the flower. The interaction between buzz-pollinated flowers and their pollinators is influenced by their physical size relative to each other, but the drivers of these size-dependent associations remain unclear. Using eight beaked louseworts (*Pedicularis*) as a model system, we combined behavioral observations, biomechanical analyses, and pollinator network analyses to test the hypothesis that the location of where a bee bites should constrain the interaction between *Pedicularis* and bumblebees during buzz pollination. We found that bumblebees always chose to bite the same site at the base of the floral beak when buzzing *Pedicularis*, and this site is optimal for transferring vibrations from the bee to release pollen from the anthers. Bee bodies must be long enough for the mandibles to clamp onto the same optimal site on the floral beak, while its pollen-collecting abdomen is positioned at the opening of the floral beak where pollen grains are ejected. Our pollination networks showed size matching between the floral beak length of each *Pedicularis* species and the body length of individual bumblebees regardless of bee species. These results suggest that the optimal excitation point on the *Pedicularis* flower links a suite of floral traits to its pollinators' dimensions, potentially contributing to prezygotic isolation among co-flowering, sympatric *Pedicularis* species.

bumblebee behavior | buzz pollination | floral vibration mechanics | *Pedicularis* | plant biomechanics | plant-pollinator interactions | trait matching

INTRODUCTION

The evolutionary success of flowering plants is linked closely to their interactions with animal pollinators. Pollinators collect resources from flowers, such as pollen and nectar, and disperse pollen onto stigmas while foraging. The capacity of floral visitors to remove and transfer pollen is mediated by both floral traits and the morphological and behavioral characteristics of the pollen vector (Latty and Trueblood, 2020; van der Kooi et al., 2021). The reciprocal adaptations between plants and pollinators often cause traits to match (e.g., the nectar inside thin and deep flower tubes is accessible only to hawkmoths with matching long tongues), promoting pollination success in plants and foraging efficiency in their pollinators (Stang et al., 2009). Furthermore, trait matching increases interaction frequencies influencing the structure of plant-pollinator networks based on degrees of coadaptation (Peralta et al., 2020). In pollination networks, the key role of morphological traits related to the size and shape of organisms has been well identified as their functions are easier to observe and measure in the field (Cantwell-Jones et al., 2024; Liang et al., 2021; Peralta et al., 2024). In contrast, the importance of biomechanical traits in pollination, i.e., those traits that mediate the mechanical interactions between flowers and pollinators, have been less well studied (Whitney and Federle,

Citation: Xu, Y., Wu, B., Vallejo-marín, M., Bernhardt, P., Jankauski, M., Li, D.Z., Buchmann, S., Wu, J., and Wang, H. Vibration mechanics involved in buzz pollination lead to size-dependent associations between bumblebees and *Pedicularis* flowers. Sci China Life Sci, https://doi.org/10.1007/s11427-024-2858-5

2013); even though these mechanical traits have long been recognized. This includes the trip mechanism in the keeled flowers of the Fabaceae and the staminal lever system in salvia flowers (Reith et al., 2004; Westerkamp, 1997). Since morphology, surface area, and internal tissues of plants and their pollinators possess multifunctional properties during pollination interactions, an assessment of their mechanical factors requires a multidisciplinary approach including laboratory tests to isolate the contribution of mechanical aspects during the plant-pollinator contact (Bauer and Poppinga, 2022; Whitney and Federle, 2013).

Buzz pollination is a specialized pollination syndrome typically integrating complex mechanical interactions between flowers and their pollinators (Vallejo-Marín, 2019). It is a widely distributed pollination syndrome incorporating more than 20,000 angiosperm species including crops like tomatoes, eggplants, and blueberries (Buchmann, 1983; Cooley and Vallejo-Marín, 2021; Vallejo-Marín and Russell, 2024). During buzz-pollination, pollinators (bees) apply high-frequency thoracic vibrations to harvest pollen that is often concealed in tubular/conical structures (e.g., poricidal anthers) (Cardinal et al., 2018; Vallejo-Marín and Russell, 2024). Buzz-pollinated flowers interact with bee pollinators through a close mechanical coupling that makes biomechanical properties of both bees and flowers particularly important, providing a good model system to study the role of biomechanical traits during pollination interaction. The morphology of buzz-pollinated flowers varies in organography, structure, and overall flower size (Dellinger et al., 2019). The flowers of congeners may present different numbers of poricidal anthers of divergent lengths and shapes (e.g., *Solanum* (Carrizo García et al., 2008; Vallejo-Marín et al., 2022)). Others show fusion (connation) of anthers forming anther cones (e.g., *Echeandia* (Bernhardt and Montalvo, 1979) and *Solanum* (Vallejo-Marín et al., 2022)). In other cases, some species in the genus *Pedicularis* retain longitudinally dehiscent stamens within a galea, an elongated and tubular hollow beak composed of connate petals (*sensu* (Macior and Sood, 1991)). Previous studies showed that flower size predicted body lengths of the most frequent species of bees pollinating flowers with poricidal anthers (Delgado et al., 2023). In addition, Corbet and Huang (2014) found that *B. friseanus* workers sorted themselves among *Pedicularis* species according to body size. It remains unclear, though, as to which mechanism drives such size-dependent correlations between bees and their buzz-pollinated host plants.

Pollen release is a function of both the properties of the flower and the characteristics of the vibrations produced and applied by the bee. Experimental studies using bee-like vibrations have shown that pollen release is positively related to the duration and amplitude (e.g., acceleration, velocity, or displacement) of the vibration applied to the flower (De Luca et al., 2013). Bees apply vibrations generated with their thoracic muscles to flowers in a variety of ways (Switzer et al., 2016), but perhaps mainly through mandible biting (King and Buchmann, 2003). Mandible biting remarkably increases the amplitude of flower vibration, potentially increasing the rate of pollen release (Woodrow et al., 2024). The point at which the bee's mandibles bite the flower is analogous to an excitation point (the point of vibration input) in a forced vibration system (Genta, 2009). In a forced vibration system composed of a flower and a bee, the response vibration is determined by a range of mechanical properties of the flower, including its architecture, morphology, material property, mass loading, and location of the excitation point (Genta, 2009). It is conceivable that a flower should have excitation points that would maximize its response to vibration when bees produce vibrations at these locations. In turn, strong flower vibrations should maximize the amount of pollen released per unit time. However, even if such points exist, a bee might not be free to exploit them as the bee needs to ensure that at least part of its body is positioned at the point in which pollen is ejected (i.e., the apical pores of poricidal anthers, or the terminal pore of the *Pedicularis*' galea) (Huang and Shi, 2013; Luo et al., 2008). The amount of pollen collected by the bee should influence its behavior and visitation patterns (Buchmann and Cane, 1989; Thorp, 2000). Thus, the location of the biting point on the flower and the dimensions of the pollen release structure may confine a bee's choice of flowers depending on its own body size. We hypothesize that the location of optimal excitation points, in combination with the size of both the flower and the visiting bee, drives a pollinator's preferences for specific flower sizes as it forages among different buzz-pollinated species.

In the present study, we address this hypothesis by recording bee behavior, including how bees manipulate and bite the flower, on eight buzz-pollinated *Pedicularis* species native to China (Figure 1D). *Pedicularis* remains one of the largest angiosperm genera with over 600 species in the Northern Hemisphere. The primary pollinators are bumblebees (*Bombus*) (Yu et al., 2015). Sympatric *Pedicularis* species often bloom at the same time sharing the same species of bumblebee pollinators (Eaton et al., 2012; Macior, 1983; Macior et al., 2001; Wang and Li, 2005). Bumblebees usually vibrate only beaked flowers of *Pedicularis* species for pollen, and forage for nectar and/or pollen on sympatric but beak-less congeners (Liang et al., 2018; Wang and Li, 2005). The tube-like beak fulfills a function similar to hollow, elongated, and poricidal anthers in other unrelated buzz-pollinated species, as pollen grains are released at the terminus of the beak following vibration (Figure 1A). Beak morphology is more variable than poricidal anthers in terms of dimension and/or shape (Figure 1C), making it an ideal model lineage to study interactions between bees and buzz-pollinated flowers. First, we construct a computational model based on the mechanical properties of real flowers. Then we assess the effects of different locations of excitation points and different bee sizes on floral vibration, using finite element analysis (FEA), a standard and powerful engineering analysis technique used to study biomechanics issues within complex structures (Richmond et al., 2005). Finally, we build a quantitative pollination network at the individual level to analyze the relationship between bee body size and floral traits under field conditions. By integrating the results from ethology, biomechanics, and ecological network analyses, we propose a mechanism driving any size-dependent correlations between bee and flower morphology in buzz-pollinated, sympatric, and co-blooming *Pedicularis* species.

RESULTS

Bumblebees bite similar floral sites when buzzing *Pedicularis* species

We assessed the behaviors of worker caste bumblebees recorded from 113 video clips. Although these *Pedicularis* species show different modes of floral presentation (Figure 1), our videos show that the buzzing behaviors of bumblebees and their biting points

https://doi.org/10.1007/s11427-024-2858-5

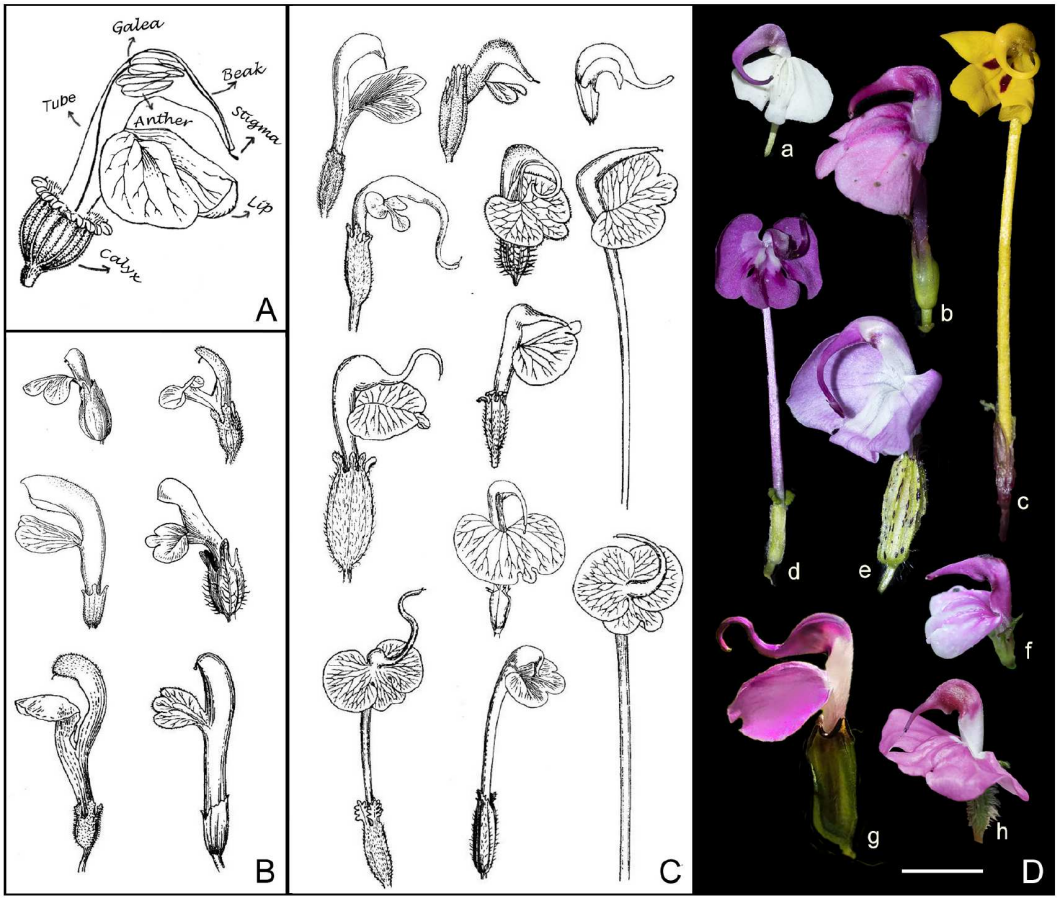

Figure 1. Flower forms of *Pedicularis*. A, Flower organography with beaked galea showing the receptive stigma protruding from the galea's beak (drawn by Xu, YQ). B, Flower forms of bilabiate species (galea lacks a beak). C, Variation in floral forms of beaked species (from Flora Yunnanica (Wu et al., 2006)). D, Flowers of eight species used in this study, bar=10 mm. a, *Pedicular oxycarpa*; b, *P. cephalantha*; c, *P. longiflora*; d, *P. milliana*; e, *P. rhinanthoides*; f, *P. axillaris*; g, *P. integrifolia*; h, *P. gruina*.

were similar regardless of plant species or field site. (Figure 2A–G). Bumblebees generally land on the left side of the flower beak. All biting sites on eight *Pedicularis* species are located where the beak connects to the body of the galea (Figure 2H). The insect uses its front and middle legs to clasp the beak and presses its abdomen to the beak's terminal opening. The thorax of the same bumblebee almost never touches the beak. Instead, when a bumblebee begins to vibrate, the pollen released from the beak's terminus is deposited on its abdomen. As this occurs, the bumblebee uses its hind legs to collect those ejected grains clinging to its abdomen (Video S1). A typical bite and sonication last 2–4 s, leaving an indentation on the galea lobe (Figure S1). Female bumblebees only buzz (sonicate) while they are biting the floral beaks.

A bumblebee's biting point is the optimal excitation point for floral vibration

The geometry model for FEA is shown in Figure 3D. According to the average value of experimental tests, the material density of the whole FEA model was set to 614.54 kg m^{-3}, and Young's modulus of the beak part, galea part and flower tube part were 169, 162.5, and 18.2 MPa, respectively, since different parts of the flower were determined to have distinct moduli.

The first FEA results show that the anther amplitude is at a maximum when excitation is applied at point 7 on the base of the galea's beak near the internal anther cluster (Figure 4B) under the simulation of two vibration excitation functions (velocity and acceleration). Hence, point 7 is the optimal excitation point of our flower model. This optimal excitation point on the geometric flower model is consistent with the actual biting indentation marks on *Pedicularis* flower left by bumblebee in the field. In the second FEA treatment, we used the equation of linear regression of mass (m) and length (L) of all bumblebees collected in the field, m=0.0269L−0.1904, R^2=0.7571 (Figure S2). The mass of small, medium, and large bumblebees is 0.107, 0.188, and 0.269 g, respectively. When the mass of the large bumblebee is loaded onto this system, it lowers the natural frequencies and changes vibration modes (Figure S3D). As the bumblebee matches the flower's beak length and bites at the optimal location on the galea, it excites the strongest beak and anther vibration displacement movements even if it uses a vibration with the same frequency and amplitude (Figure 4E).

The experimental results show that, under vibrations with the same frequency and velocity, the beak's response to excitation at point 6 is about 0.60 of the value at point 7 (y=0.5973x, R^2=0.9053). This linear regression model is significant at the 0.001 level ($F_{(1,3)}$=38.014, P<0.001). The simulation results from FEA suggest that the response of the beak from excitation at point 6 is about 0. 43 of the one at point 7 (y=0.4271x, R^2=1). Although the effects differ somewhat between the experimental and FEA results, both are consistently showing that point 7

Figure 2. Foraging positions and biting points of bumblebees during buzzing seven *Pedicularis* species. A–G, *B. festivus* on *P. cephalantha*; *B. nobilis* on *P. integrifolia*; *B. friseanus* on *P. gruina*; *B. friseanus* on *P. oxycarpa*; *B. festivus* on *P. rhinanthoides*; *B. friseanus* on *P. longiflora*; *B. ladakhensis* on *P. milliana*. H-1 and H-2, Flowers of *P. rhinanthoides* with galea structure and anther cluster. Arrows indicate the locations of the biting points.

results in a much stronger vibration response to the flower's beak (Figure S4). Results predicted by FEA simulation agree qualitatively with the floral experiments using *P. integrifolia*.

Trait matching of bumblebees and flowers

We collected and identified 179 individuals, which represent 9 bumblebee species foraging on all 8 *Pedicularis* species (see the frequency of interactions in Figure 5). The mean values of 3 bumblebee body traits and 6 floral traits measured are listed in Table S1. At the species level, the results of fourth-corner analysis involving all trait pairs show that a marginally significant trait matching ($P<0.05$) occurs between the in- and out-linear length of the galea beak with bee body length and the ITD of each bumblebee species (Figure 6A).

At the individual level, the distribution of trait ratios of floral traits of *Pedicularis* species to the body lengths of their visiting bumblebees shows that the trait-pairs relating to beaks present a bell-shaped curve. This suggests that rather than flower tube length and lip width, the interaction of bumblebee with flower species is mainly influenced by the traits of flower beak (Figure 6B). Although the four traits of beak are self-correlating, the results show that the distribution of the ratio between in-linear beak length to bumblebee body length has the highest density and the sharper peak. Its variance, skewness, and kurtosis are closer to zero than others. This suggests that the distance between the biting point to the open end of the beak affected interaction frequency between the bumblebee and its *Pedicularis* flower more strongly. The ratio of this trait pair distributes bias less than 1.0, indicating that a bumblebee prefers to visit a flower that has a beak length shorter than its own body length. Additionally, despite the random effects of bumblebee species, we still found evidence of a significantly positive relationship between a bumblebee's individual body length and the linear length of the galea beak (GLMM: $F_{(3,175)}=27.694$, $P<0.001$). The above evidence suggests trait-matching between a flower's beak and the body length of its foraging bumblebee visitors.

DISCUSSION

When bumblebees buzz these *Pedicularis* flowers, their vibrations should be transmitted to the flower mainly by mandible biting due to the immediate connection between every bee's head and its thorax (King and Buchmann, 2003). Our observations suggest that a bumblebee's choice of a biting location does not occur at random. Biting locations are located at the base of the galea's beak just above the anther cluster, which coincides with the best excitation point predicted by our FEA model. As pollen release relates positively with amplitude (De Luca et al., 2013; Kemp and Vallejo-Marín, 2021; Rosi-Denadai et al., 2020), a bumblebee that bites on the optimal excitation point should remove most pollen compared to other locations on the same flower. The consistency between a bumblebee's choice of biting locations and the optimal location of the excitation point in our FEA model shows the impact of floral biomechanical properties on bumblebee behavior.

Although *Pedicularis* flowers have an optimal excitation point for pollen release, not all bees are able to exploit it due to one simple factor. The abdomen of a vibrating bee must be able to receive the pollen ejected at the tip of the galea while its mandibles remain clamped to the optimal excitation point. If pollen is deposited on parts of its body that are least accessible during grooming (e.g., the dorsum of its thorax or the petiole between its thorax and abdomen) (Koch et al., 2017), or if grains are discharged into mid-air without reaching the bee's body, then the amount of pollen collected must decline. The ventral side of a bee's abdomen is one of the most accessible parts during pollen grooming (Koch et al., 2017), which probably explains

https://doi.org/10.1007/s11427-024-2858-5

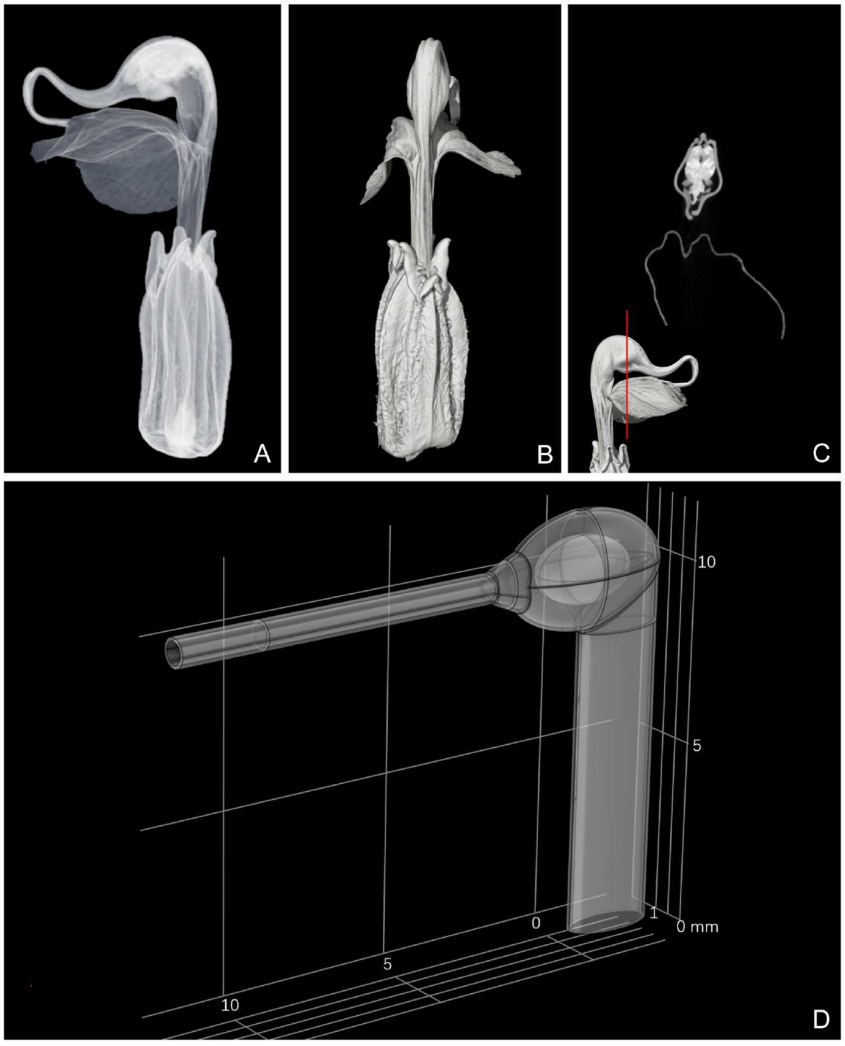

Figure 3. Morphology of the real beaked *Pediculairs* flower and the geometric model of the flower. A–C, Micro XCT images of *Pedicularis integriflolia* as an example showing the translucence view, back side view, and cross-section and close-up of an anther cluster. D, Geometric model for the FEA. Specifically, the shell thickness was 0.1 mm, the beak was a 10 mm long and 0.8 mm wide tube, the galea's shell was 4.9 mm×2.1 mm×3.2 mm, the anther ellipsoid was 2.8 mm×1.8 mm×2.8 mm, and the flower's oblate tube was 1.2 mm×2.5 mm.

why bumblebees curl their bodies into a C-shape around the terminal opening of any *Pedicularis* beak (Figure 1; Video S1). As the lengths of floral beaks vary among different *Pedicularis* species, only bees of the size (length) matching that beak length can apply their vibrations simultaneously at the optimal excitation point while collecting pollen from the galea's terminus. As a consequence, a bee's body length should constrain its ability to harvest *Pedicularis* pollen, similarly as its proboscis length constrains its ability to suck nectar from elongated floral tubes or spurs of varying lengths in other angiosperm species (Liang et al., 2021). This hypothesis is supported by our pollination network analyses. All bumblebee species show a wide range of intraspecific variations in body size and are not species-specific when visiting *Pedicularis* (Figure 5). However, trait-matching occurs between bee body length and floral beak's linear length not only at the species level but also significantly at the individual level. This suggests that an individual bumblebee chooses a *Pedicularis* species depending mainly on its own relative body length and relative lengths of floral beaks of *Pedicularis* flowers rather than other floral traits. Thus, our findings show that the excitation point should play a role in mediating size-dependent correlations between bees and beaked galea of different *Pedicularis* species, providing a good example of how a few but very specific floral traits shape plant-pollinator interactions during buzz pollination.

Our study raises the possibility that changes in floral traits within a buzz-pollinated lineage allow sympatric and co-blooming plants to exploit co-occurring bees of different sizes. Generally, bumblebees are generalist (polylectic) pollen foragers (Grant, 1950). Although buzz pollination behavior is a specialized system, buzz-pollinated plants are often co-blooming and share the same pollinator species (González-Vanegas et al., 2021). In sympatric *Pedicularis* species, size-matching associations at the individual level could facilitate pre-pollination reproductive isolation even though they are pollinated by the same bumblebee species. Previous authorities suggest that pollinator floral constancy is the key pre-pollination barrier in co-blooming *Pedicularis* (Liang et al., 2018; Tong and Huang,

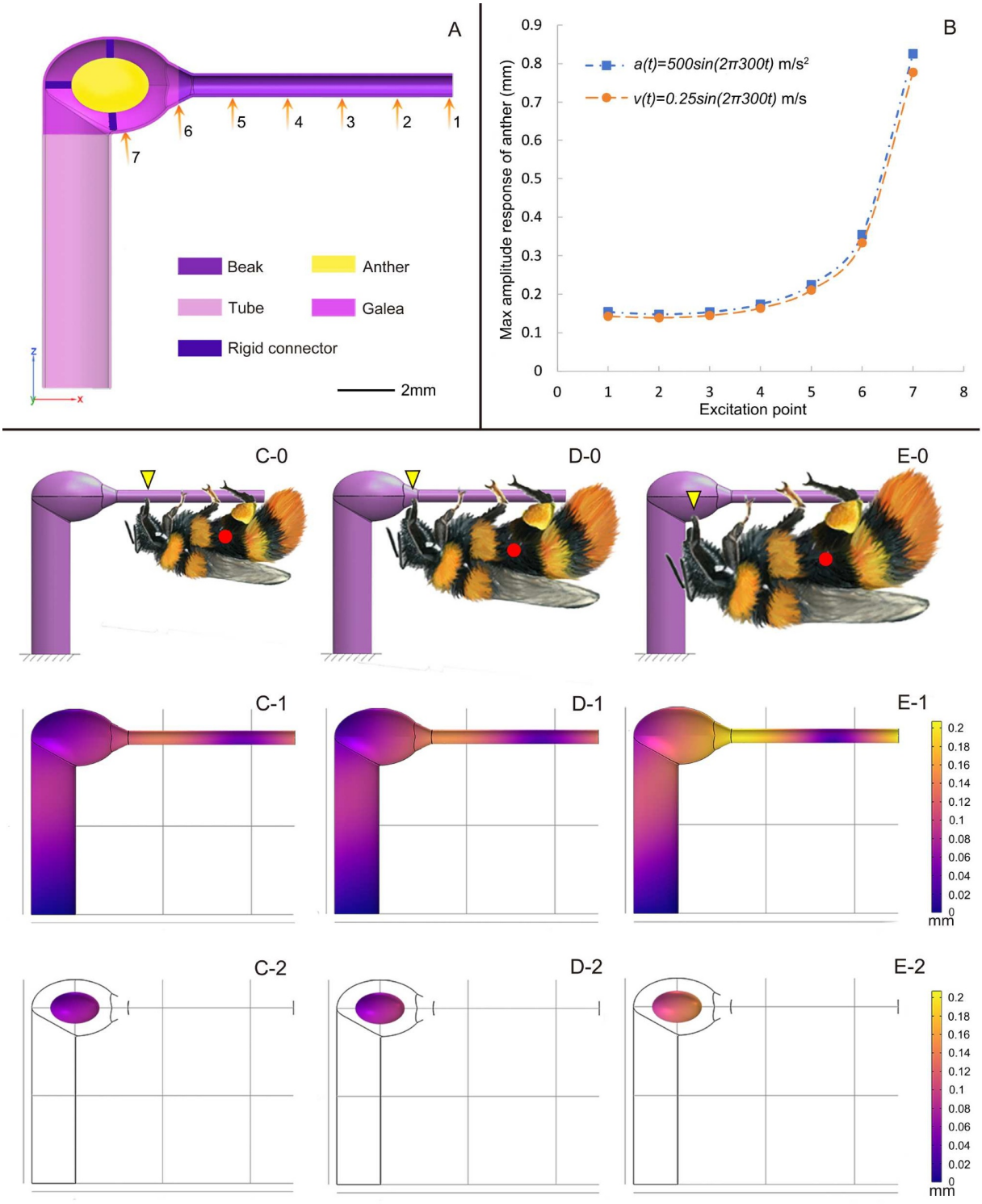

Figure 4. The effects of biting points on the bee-flower vibration system of beaked *Pedicularis*. A, The computational model of a beaked *Pedicularis* flower. Arrows show the excitation points' location and direction. Bar=2 mm. B, The maximum amplitude of the anther ellipsoid in the *z* direction of each point under excitation. C–E, Vibration response via FEA for *Pedicularis* flowers with bees of different sizes (C, Small, D, Medium, E, Large) under the same forcing vibration function. The yellow triangle and red dot in C-0, D-0, and E-0 show the excitation point and center mass, respectively. C-1 to E-1 are the responses of the respective flower with C-2 to E-2 as the responses of the respective anther ellipsoid.

2016). During a foraging bout, individual bumblebee workers rarely forage more than one *Pedicularis* species, which reduces the possibility of interspecific crosses caused by heterospecific pollen loads. Our results augment the understanding of factors influencing flower constancy. Bumblebee workers produced in the same nest vary greatly in physical parameters including body length, thorax width, and proboscis length (Peat et al., 2005). The body lengths of bumblebee workers from the same colony

https://doi.org/10.1007/s11427-024-2858-5

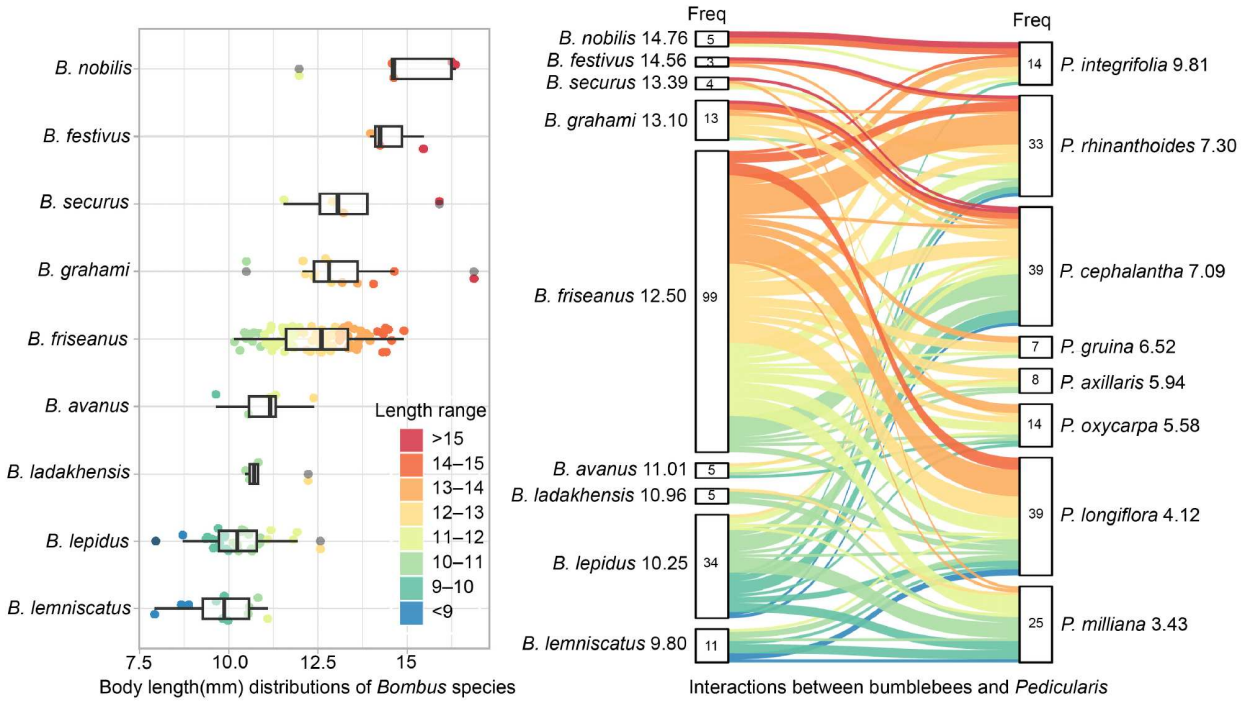

Figure 5. The body length (mm) distributions of each visiting bumblebee species and their interaction frequencies with each *Pedicularis* species. The body length range of each bee individual is marked in color. The links are interactions between bumblebees and plants, line thicknesses are proportional to the number of interactions. The corresponding interaction frequencies are given in boxes. From top to bottom, bumblebee species are ranked by mean body length, and *Pedicularis* species are ranked by mean beak in-linear length in a descending order. Values are shown alongside their names.

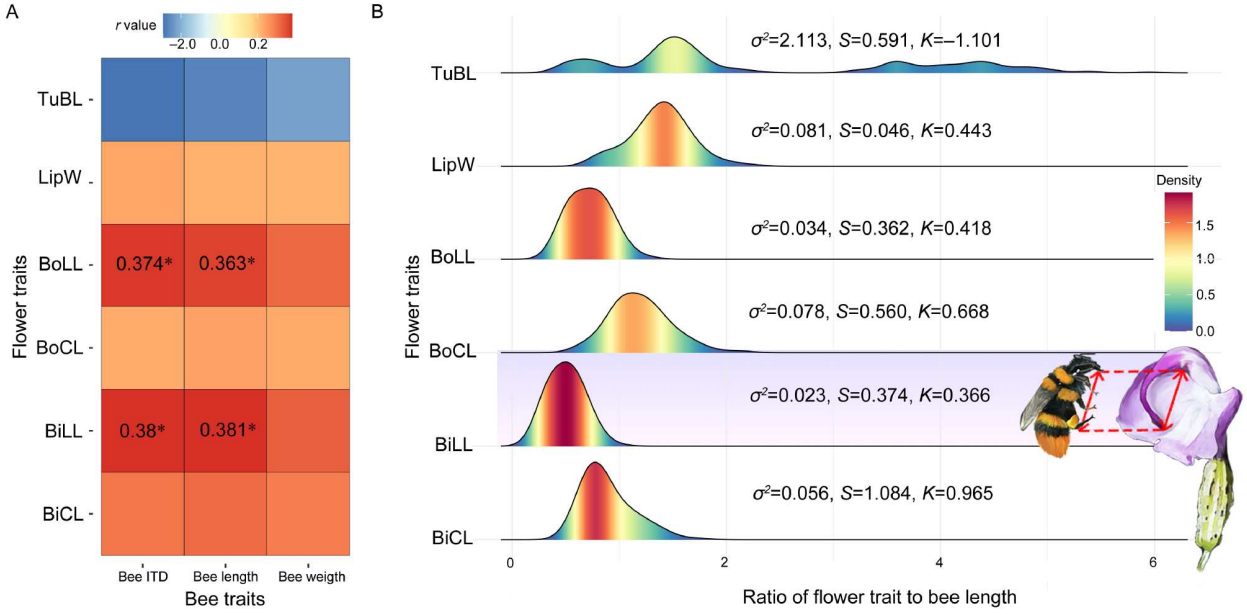

Figure 6. Results of trait matching analyses. A, Fourth-corner analysis results for relationships between floral and bee traits. Boxes are colored according to the fourth-corner coefficients (*r* value) of the trait-pairs; the asterisk (*) marks the trait pairs with significant relationships ($P<0.05$). B, Distribution of trait ratios of the floral traits of *Pedicularis* species to the body lengths of visiting individual bumblebees fitted by kernel density estimation method. The variance (σ^2), skewness (S), and kurtosis (K) of each distribution are listed. TuBL, flower tube length; LipW, low lip width; BoLL, out linear length of flower beak; BoCL, out curve length of flower beak; BiLL, in linear length of flower beak; BiCL, in-curve length of flower beak. The polygon shows the matching trait pairs.

might restrict their choices among different, co-blooming *Pedicularis* species based upon the best excitation point and the variation in floral beak length. In turn, individual bumblebees belonging to different species but with similar body lengths can pollinate the same *Pedicularis* species. This kind of morphological matching should promote pollinator niche partitioning (Lautenschleger et al., 2021), while reducing heterospecific pollen deposition, otherwise resulting in either failed pollination or

interspecific hybridization.

Trait-matching caused by the optimal excitation point can be interpreted as a consequence of reward economics and bee foraging decisions. Learning how to forage for pollen represents a substantial time investment for individual foragers (Raine and Chittka, 2007) and buzz pollination represents a complex skill. During field observations, we saw that the pollen foraging of some bumblebee individuals on the flowers was less adept than others. Therefore, in the presence of multiple *Pedicularis* species, each forager must learn where to bite different flowers to locate the best excitation point. Learning cost compels an experienced bee to visit flowers it has learned previously to manipulate (Russell et al., 2016). The economic decision about which flowers to visit facilitates patterns of floral constancy (Gegear and Thomson, 2004; Heinrich, 2004) and may explain why pollen-foraging bumblebees are more constant to buzz-pollinated flowers compared to sympatric, nectar-secreting flowers (Macior and Sood, 1991). Therefore, variation in floral traits of buzz-pollinated plants may facilitate an ethological isolating mechanism among co-blooming members of the same genus by enhancing floral constancy. Further field experiments on pollinator ethology will help us understand how floral diversification evolves within a plant lineage where most species appear dependent on the same pollinators.

Matching between corolla size and their pollinator's body size occurs in other buzz-pollinated plants with poricidal anthers (Delgado et al., 2023). However, we still do not know whether the excitation point also acts as a selective mechanism driving size-dependent correlations between highly modified poricidal anthers and their bee visitors in those taxa. A study on *Solanum* flowers found that the angle with which the bee bites the anther can induce different displacements of the major vibrational axes of the anther (Woodrow et al., 2024). Moreover, the location and magnitude of bee mass loading onto the poricidal anther change the natural frequencies and vibrational modes (Jankauski et al., 2022). Shifts in the location of the biting point will cause changes at the center of bee mass on poricidal flower structures, influencing the vibrational response of a poricidal anther during bee sonication. The modification of organ architectures and anther connective appendages in flowers with poricidal anthers also have a strong influence on vibration transmission and pollen release under buzzing (Bochorny et al., 2021; Nevard et al., 2021; Vallejo-Marín et al., 2022). It is reasonable to assume that other buzz-pollinated flowers with different structures possess excitation points and/or areas associated with maximum vibration transmission and a resonance response. Applying computational floral model analyses on these untested flowers will help us to understand how excitation points may affect plant-pollinator interactions in buzz-pollinated species unrelated to *Pedicularis*.

The FEA method has been applied successfully to the structural dynamic of *Solanum* stamens (Jankauski et al., 2022). Nevertheless, beaks of *Pedicularis* and poricidal anthers of other buzz-pollinated species vary in length, shape, curvature, ornamentation, degrees of twisting, and other morphological/physical factors. To investigate how these modifications may influence floral vibration dynamics requires more complex FEA models. Unfortunately, FEA cannot fully explain the pollen-release mechanism during buzzing. The pollen release process is important to understand the pollinator's behavior, but how it is influenced by floral traits is not clear (Bochorny et al., 2021; Buchmann and Hurley, 1978; Vallejo-Marín, 2019; Vallejo-Marín et al., 2022). It is quite a challenge to describe the movement of pollen grains under vibration as it involves complex physical theories (Buchmann and Hurley, 1978; Corbet and Huang, 2014; Hansen et al., 2021). As the movement of pollen grains is similar to particle motion within a vibrating tube (Sánchez et al., 2009), numerical simulations based upon the discrete element method (DEM) could become a potential computational modelling method for studying pollen ejection during buzz pollination in the future (Boucher-Bergstedt et al., 2024; Guo et al., 2019).

CONCLUSION

Our multidisciplinary study shows the important role of the location where a bee bites in shaping plant-pollinator interactions during buzz pollination. Due to the location of the optimal excitation point in the flower and variation in a bee's body size, variation in floral traits among closely related species of buzz-pollinated plants enables the assortment of floral visitors of different sizes when congeners are sympatric and co-blooming. This type of bee-flower trait matching may further contribute to ethological isolation while lessening competition among co-blooming and buzz-pollinated species dependent upon the same pollinator species. Our study suggests that variation in floral traits affecting the biomechanical interaction between flowers and their visitors may both contribute to and sustain floral diversification.

MATERIALS AND METHODS

Species and study sites

This study was conducted in the Shangri-La and Lijiang counties of Yunnan Province in southwestern China, from July to early September, in 2021 and 2022. We chose eight beaked *Pedicularis* that do not secrete nectar and differ in beak morphology, flower tube length, and corolla color. These species are all visited by pollen-foraging bumblebees (Table S2). The beaks (see Figure 1A for terminology of floral structures) of *P. axillaris* Franchet ex Maximowicz, *P. oxycarpa* Franchet ex Maximowicz, *P. gruina* Franchet ex Maximowicz and *P. cephalantha* Franch. are slightly falcate and differ in length and angle of bending. Yellow-flowered *P. longiflora* Rudolph and pink-flowered *P. milliana* W. B. Yu, D. Z. Li & H. Wang have very narrow and elongated flower tubes with semicircular beaks. Pink-flowered *P. integrifolia* J. D. Hooker and pale, pink-flowered *P. rhinanthoides* Schrenk ex Fischer & C. A. Meyer possess long and curved S-shaped beaks (Figure 1D). Except *P. gruina* and *P. integrifolia*, all species are sympatric within study sites. Co-blooming mixed patches of *P. longiflora*, *P. cephalantha*, and *P. rhinanthoides* were observed in wet meadow habitats, while *P. milliana* flowered along wetland edges. *Pedicularis. milliana*, *P. oxycarpa*, and *P. axilaris* flowered together along moist forest edges.

Video tracking and analysis of the pollination behavior

While workers and queens forage together on *Pedicularis* species, we did not discriminate between them. We used a custom three-camera video recording system to register buzzing behavior. We applied three GoPro cameras (HERO9 Black, GoPro, Inc.,

https://doi.org/10.1007/s11427-024-2858-5

California, USA) on a custom-made 3D-printed holder with three heads to obtain top, side, and front views of bumblebees as they visited flowers. Using our videos in .mp4 format, we recorded where individual bumblebees bit the flower and the portion of the bumblebee's body that contacted the terminus of the galea's beak (and floral stigma) during bouts of floral vibration.

Computational model construction

Geometric parameters. The simplified geometric model mirroring *Pedicularis integrifolia* was built by the software Solidworks (version 2020). Based on our initial observations, we noticed that the lower lip of the corolla did not interact with bumblebees during buzzing, therefore our simplified geometric model dispensed with the lower lip. The exterior of the flower was modelled using thin shell elements and consisted of a round tube as the "beak", an oblate tube as the "flower tube", and an ellipsoidal shell as the "galea". The size and proportion of the structure of this simplified model were based on the average value obtained by measuring. We measured the length, width, and height of the galea and the length, width, and height of its anthers. Petal thickness, and the internal and external diameters of cross sections of both the beak and floral tube were also measured. All measurements were made with a vernier digital caliper to an accuracy of 0.01 mm. We combined the Micro-CT images and anatomy observations to determine the internal and external structures of the geometric model (Figure 3A–C). As the four stamens in a *Pedicularis* flower are fused (adnate) to the floral tube and are held parallel to each other while sheathed inside the galea shell, our simplified model used one homogeneous ellipsoid representing all anthers. In a real flower, all anthers are wrapped together within the galea sheath, fixing their positions within the galea's shell (Figure 3C). Thus, the vibration of the galea shell is transferred to all the anthers upon contact at the same time and their combined vibration is complicated. To simplify these motions, we used rigid connector elements to link the sheath and the anther ellipsoid (see Figure 4A).

Material properties. We applied indentation measurement on the epidermal cells of the different petal parts to assess the Young's modulus of flower petal, as the epidermal cells of petals of *Pediculairs* flowers in the beak, galea, flower tube, and lips have distinctive features (unpublished data). Indentation measurement can reflect the heterogeneous physical properties of this kind of soft tissue (McKee et al., 2011). We cut 2 mm×3 mm fragments from the galea, beak, and floral tube of fresh flower petals for measurements. The specimens were indented using an atomic force microscopy (AFM) instrument (Bruker, Dimension Fast Scan Bio, Germany) equipped with a probe (RTESP-300, Bruker) with an average indentation depth of 0.15 μm. To prevent desiccation, indentations were made immediately after the petal fragments were separated from the flower. The Young's modulus was determined in NanoScope Analysis 2.0, based on force-displacement curves (FDCs). Material density was determined by the average mass and the petal's volume. Whole petals were dissected from 20 fresh and fully opened flowers. Each petal was weighed on an electronic scale to obtain the average mass. For petal volume, we used a nanoVoxel-2000micro-CT scanner (Sanying Precision Instruments, Tianjin, China) at 45 kV and 500 μA to obtain 3D reconstructions. We then segmented the whole petal from the initial reconstructions and further analyzed the volume of petal segmentation by Avizo 9.0.1 (Thermo Fisher Scientific, USA). The average mass divided by the volume of the petal is the material density of that petal.

Finite element analysis

We applied computational modelling (FEA) to study the effects of different biting locations on the bee-flower vibration system. It was conducted using the software COMSOL Multiphysics (version 6.0). In the simulation process, the Newton-Raphson linear method was used. We assumed that the flower had linear-elastic and isotropic material properties. We set the density and the Young's modulus according to the experimental measurements. The Poisson's ratio of the entire structure was set to 0.45, as in pumpkin floral tissue (Shirmohammadi et al., 2017). The anther ellipsoid was treated as a rigid body and was not deformable. The bottom surface or shell of the flower tube was regarded as constrained and fixed as the boundary condition of the system. The remainder of the model had no position, velocity, or acceleration constraints except for the excitation point.

A forcing function (function of excitation force, representing the vibrations generated by the bee) was set according to observed values of bumblebees' pollination buzzes as described below. We used a pure-tone sinusoidal vibration. The forcing functions were set as a one-dimensional simple harmonic in time. We set the excitation vibration frequency at 300 Hz which is an approximate value of floral buzzing by bumblebees on *Pedicularis* flowers. Using the maximum amplitude of the vibration velocity and the maximum amplitude of acceleration recorded from *Bombus terrestris* (Pritchard and Vallejo-Marín, 2020), we set two different vibration excitation functions. The first relationship was between the velocity of the given excitation points with the time described as $v(t)=0.25\sin(2\pi 300t)$ m s^{-1}. The second was the relationship of the acceleration of the given excitation points with time described as $a(t)=500\sin(2\pi 300t)$ m s^{-2}. The frequency and the amplitude excitation functions were the same during all simulations. Prior to simulations, the flower model's natural frequencies and mode shapes were scrutinized to prevent resonance induced by the 300 Hz bumblebee floral buzzing frequency (see SI and Figure S3).

Based on our field observations, we conducted two simulation studies to determine how variable excitation points affect the flower's vibration. As the amplitude of bee-mediated vibrations is the main determinant of the amount of pollen released when flowers are buzzed (De Luca et al., 2013; Kemp and Vallejo-Marín, 2021; Vallejo-Marín, 2019), we utilized the amplitude of flower vibration as the primary metric for assessment. First, we assessed how different excitation points affected the vibration of the anther ellipsoid. The dependent variable was the simulation calculation value of the maximum amplitude of the anther. As a buzzing bumblebee bites the galea with its mandibles and presses the beak terminal to its abdomen, the continuous galea-beak unit was defined here as the feasible region of excitation points. In the symmetry plane of the flower model, we set the opening of the beak as the center and drew circles with radii of 0, 2, 4, 6, 8, 10, and 12 mm on the feasible region. The intersections of seven circles with the lower surface of the flower model were excitation points. All excitation forces were in z-direction (see Figure 4A). Second, we analyzed the vibration modes of the flower with different bumblebee sizes. We loaded in "bumblebee mass" with different body lengths on flowers and applied simulated vibrations to corresponding biting points. According to the statistics of

real visiting bumblebees on *Pedicularis* species, we chose three body lengths (11, 14, and 17 mm) corresponding to small, medium, and large bumblebees. Their body mass was estimated by the equation of linear regression between body mass and body length of the collected bumblebee specimens. As buzzing bumblebees use their abdomens to collect pollen, we assumed that the contact point to the galea beak opening was located at seven-tenths of the length of the bumblebee's body, while the biting point was located at the front of the bumblebee's head. Hence, the biting point of each bumblebee was closer to points 5, 6, and 7 of the previous simulation. The location of each center of mass point and excitation point is shown in Figure 4C-0, D-0 and E-0. We treated the bumblebee as a point mass and set gravity (g=9.81 m s^{-2}) in a negative z direction. The locations of the center of mass and the biting point (excitation point) were determined using this premise. The same vibration was applied to analyze the vibration modes of the whole flower and the anther ellipsoid under the loading conditions of the three bumblebee sizes.

Vibration experiment on fresh flower

To further validate the results from FEA, we performed vibration experiments on the fresh flowers of *P. integrifolia*. Its morphology most resembles the geometric model we constructed, and the vibration direction of bumblebee visitors is in accordance with the excitation direction considered in the FEA model. Whole inflorescences were collected from our field sites and kept moist in sealed plastic bags. They were brought to the lab in less than one hour. During the whole experiment, an inflorescence was kept fresh by placing its cut end into the water of a Currie fresh flask. Only freshly opened and unvisited flowers were chosen for experiments. The lip of the flower was removed. We used a mini-shaker (SINOCERA Piezotronics, China) to produce vibrations in 300 Hz sine wave. The vibration was transmitted to the flower by a custom-made tweezer (3D printed) in the z direction. The tweezer clamped the flower in a manner analogous to how a bumblebee bites a flower when it performs floral buzzing. We set velocity amplitudes of 50, 100, 150, and 200 mm s^{-1}. The input amplitude of the tweezer was adjusted by a Power Amplifier (SINOCERA Piezotronics), and was monitored by a laser vibrometer (Polytec GmbH, Germany). We input vibration at the sites corresponding to points 6 and 7 in the geometric flower model and recorded responses (amplitude) of the beak's front end (corresponding to point 2, Figure 4) with a laser vibrometer (Polytec GmbH) in the z direction (Figure S5). The amplitude and frequency were recorded by VibSoft5.5 (Polytec GmbH). Each inputting velocity measurement was taken three times for each flower (n=12 flowers). For each flower, excitations were applied on points 6 and 7, and the floral beak's vibrations were recorded pairwise for comparison. We also simulated vibration with the same velocity and frequency on the sites (point 6 and point 7) in the FEA model, recording the amplitude of point 2. Linear regression models were built to describe the vibration responding difference between points 6 and 7 during both the experiment and the FEA. The coefficients of the two equations of linear regression were compared to qualitatively validate the FEA model.

Function traits of flowers and bumblebees

To detect whether the optimal biting location affects interactions between bumblebees and *Pedicularis* flowers *in situ*, we collected bumblebees visiting each *Pedicularis* species on sunny days and recorded the flower species on which they were caught. The interaction matrixes were formulated at the species and individual levels. We measured three traits for each bumblebee specimen: intertegular distance (ITD), body length, and body weight (Figure S6). Each bumblebee was placed in a separate 5ml centrifuge tube, and then capped and labelled. We euthanized them in the station's freezer units. To weigh each specimen, the body was first cleaned of external pollen loads using small brushes until contrasting pollen was not visible to the human eye. Nectar stored in the bumblebee's crop was extruded into a cotton swab by a slight, manual press to the bee's venter from the thorax to the terminus of its abdomen. The specimen was weighed on a microbalance precise to 0.0001 g. After measuring, bumblebees were pinned, labelled, and deposited in our collection at the Kunming Institute of Botany, Chinese Academy of Sciences, Kunming, Yunnan Province, China. All bees were identified by our laboratory staff based on long-term studies of bumblebees using the *Bombus* identification key provided by Dr. Paul Williams of the British Museum (Williams, 2022). We measured six morphological traits of 20 flowers for each *Pedicularis* species (Figure S7). As the galea beak interacts directly with bumblebees during buzzing, we measured four morphological/dimensional traits. This included the out- and in-linear lengths versus the out- and in-curve lengths. The flower's lower lip width and the floral tube length were measured as they are also important function traits during interactions between bumblebees and flowers.

Statistical analysis

We analyzed matching traits between flowers of *Pedicularis* species and bumblebee bodies and the effects of trait matching on pollination interactions at the species and individual levels. At the species level, we used fourth-corner analysis to test if a morphological trait matching explains interaction patterns. Fourth-corner analysis tested the relationships between species traits and environmental variables (Dray and Dufour, 2007). In a pollination interaction, floral traits are the environmental variables for each pollinator species. Therefore, the fourth-corner method can analyze the link between flower traits and pollinator traits (Liang et al., 2021). The mean trait values of each species, consisting of more than 3 individuals, were used in this analysis. Three matrices were constructed as follows: (i) a *Pedicularis* flower trait matrix (**R**), (ii) a *Pedicularis*-bumblebee species interaction matrix (**L**) and (iii) a bumblebee trait matrix (**Q**). The fourth-corner approach measured the link between these three matrices. The analysis was conducted by the R package ade4 (Dray and Dufour, 2007). After performing multivariate statistics that measure the global association among **R**, **L**, and **Q** (using randtest.rlq functions on permutational models 6 with 49,999 Monte Carlo permutations for a better control of type I errors), we applied the fourth-corner tests to evaluate the statistical significance of the associations between bee traits and flower traits. P values were adjusted for multiple comparisons using the FDR procedure (ter Braak et al., 2012). At the individual level, we compared the frequency distribution of the ratios of each flower trait to the bee's body length to identify the matching traits. The information on the shapes of species' frequency distributions of functional traits can show how trait

https://doi.org/10.1007/s11427-024-2858-5

overlap between plants and pollinators predicts the likelihood of their interactions (Cantwell-Jones et al., 2024). Since bees use their mandibles to convey vibration but use their abdomens to collect pollen, the bee's body length should be the key trait to obtaining pollen. If a bumblebee chooses a *Pedicularis* flower according to whether its body length matches the floral beak length, we might predict that the ratio of this trait pair distributes more intensively around some value and the shape of its distribution is near a normal shape. The distribution densities of the ratio of each trait pair were estimated by Kernel density estimation (KDE) (Carmona et al., 2019). The variance, skewness, and kurtosis of the distribution were compared to further illustrate the differences between the distribution shapes of each trait pair. Additionally, based on the two analyses above, we fitted generalized linear mixed models (GLMMs) to the candidate trait pairs to examine whether the trait matching remained significant at the individual level when considering bumblebee species identity as a random effect. Here, we set individual bumblebee body length as the predictor variable, and the mean linear length of the flower's beak as response variables, because the results of fourth-corner analysis and the frequency distribution of the ratios show that both the in- and out-linear lengths of the flower beak significantly correlated with bumblebee body length. As the response variables were Gaussian distributed (Shapiro-Wilk test: W=0.966, P=0.867>0.05), we used Gaussian distribution in the model. Analysis was conducted with two R packages the lme4 (Bates et al., 2015) and the effects (Fox and Weisberg, 2018).

Data and materials availability

The data that support the findings of this study are openly available in Science Data Bank at https://doi.org/10.57760/sciencedb.16998.

Compliance and ethics

The authors declare that they have no conflict of interest.

Acknowledgement

This work was supported by the Strategic Priority Research Program of the Chinese Academy of Sciences (XDB31000000), the Special Foundation for National Science and Technology Basic Research Program of China (2021FY100200), the National Natural Science Foundation of China (32071670). MVM was partially supported by a research grant from the Human Frontier Science Program (RGP0043/2022). This work was also partially supported by the National Science Foundation under awards No. CMMI-2221908 to MJ. We thank Yanhui Zhao, Jiangkun Wei, Haidong Li, Caiyi Fan, Qiujie Zhao, and Yi Tao for their assistance during experiments, and thank Zongxin Ren and Yanhui Zhao for their helpful advice on the research process. We dedicate this paper to the memory of Lazarus W. Macior (1926–2007), a distinguished professor at the University of Akron (Ohio) and a pioneer in the pollination ecology of *Pedicularis* species by bumblebees.

Supporting information

The supporting information is available online at https://doi.org/10.1007/s11427-024-2858-5. The supporting materials are published as submitted, without typesetting or editing. The responsibility for scientific accuracy and content remains entirely with the authors.

References

Bates, D., Mächler, M., Bolker, B., and Walker, S. (2015). Fitting linear mixed-effects models using lme4. J Stat Soft 67, 1–48.

Bauer, U., and Poppinga, S. (2022). New insights and opportunities from taking a biomechanical perspective on plant ecology. J Exp Bot 73, 1063–1066.

Bernhardt, P., and Montalvo, E.A. (1979). The pollination ecology of *Echeandia macrocarpa* (Liliaceae). Brittonia 31, 64–71.

Bochorny, T., Bacci, L.F., Dellinger, A.S., Michelangeli, F.A., Goldenberg, R., and Brito, V.L.G. (2021). Connective appendages in *Huberia bradeana* (Melastomataceae) affect pollen release during buzz pollination. Plant Biol 23, 556–563.

Boucher-Bergstedt, C., Jankauski, M., and Johnson, E. (2024). Buzz pollination: investigations of pollen expulsion using the discrete element method. bioRxiv, 2024.2008.2001.606085.

Buchmann, S.L. (1983). Buzz Pollination in Angiosperms. New York: Van Nostrand Reinhold Company. 73–113.

Buchmann, S.L., and Cane, J.H. (1989). Bees assess pollen returns while sonicating *Solanum* flowers. Oecologia 81, 289–294.

Buchmann, S.L., and Hurley, J.P. (1978). A biophysical model for buzz pollination in angiosperms. J Theor Biol 72, 639–657.

Cantwell-Jones, A., Tylianakis, J.M., Larson, K., and Gill, R.J. (2024). Using individual-based trait frequency distributions to forecast plant-pollinator network responses to environmental change. Ecol Lett 27, e14368.

Cardinal, S., Buchmann, S.L., and Russell, A.L. (2018). The evolution of floral sonication, a pollen foraging behavior used by bees (Anthophila). Evolution 72, 590–600.

Carmona, C.P., de Bello, F., Mason, N.W.H., and Lepš, J. (2019). Trait probability density (TPD): measuring functional diversity across scales based on TPD with R. Ecology 100, e02876.

Carrizo García, C., Matesevach, M., and Barboza, G. (2008). Features related to anther opening in *Solanum* species (Solanaceae). Bot J Linn Soc 158, 344–354.

Cooley, H., and Vallejo-Marín, M. (2021). Buzz-pollinated crops: a global review and meta-analysis of the effects of supplemental bee pollination in tomato. J Economic Entomol 114, 505–519.

Corbet, S.A., and Huang, S.Q. (2014). Buzz pollination in eight bumblebee-pollinated *Pedicularis* species: does it involve vibration-induced triboelectric charging of pollen grains? Ann Bot 114, 1665–1674.

De Luca, P.A., Bussière, L.F., Souto-Vilaros, D., Goulson, D., Mason, A.C., and Vallejo-Marín, M. (2013). Variability in bumblebee pollination buzzes affects the quantity of pollen released from flowers. Oecologia 172, 805–816.

Delgado, T., Leal, L.C., El Ottra, J.H.L., Brito, V.L.G., and Nogueira, A. (2023). Flower size affects bee species visitation pattern on flowers with poricidal anthers across pollination studies. Flora 299, 152198.

Dellinger, A.S., Chartier, M., Fernández-Fernández, D., Penneys, D.S., Alvear, M., Almeda, F., Michelangeli, F.A., Staedler, Y., Armbruster, W.S., and Schönenberger, J. (2019). Beyond buzz-pollination—departures from an adaptive plateau lead to new pollination syndromes. New Phytol 221, 1136–1149.

Dray, S., and Dufour, A.B. (2007). The ade4 package: implementing the duality diagram for ecologists. J Stat Soft 22, 1–20.

Eaton, D.A.R., Fenster, C.B., Hereford, J., Huang, S.Q., and Ree, R.H. (2012). Floral diversity and community structure in *Pedicularis* (Orobanchaceae). Ecology 93, S182–S194.

Fox, J., and Weisberg, S. (2018). Visualizing fit and lack of fit in complex regression models with predictor effect plots and partial residuals. J Stat Soft 87, 1–27.

Gegear, R.J., and Thomson, J.D. (2004). Does the flower constancy of bumble bees reflect foraging economics? Ethology 110, 793–805.

Genta, G. (2009). Forced response of conservative nonlinear systems. In: Genta, G. ed. Vibration Dynamics and Control. Mechanical Engineering Series. Boston: Springer. 481–499.

González-Vanegas, P.A., Rös, M., García-Franco, J.G., and Aguirre-Jaimes, A. (2021). Buzz-pollination in a tropical montane cloud forest: compositional similarity and plant-pollinator interactions. Neotrop Entomol 50, 524–536.

Grant, V. (1950). The flower constancy of bees. Bot Rev 16, 379–398.

Guo, Y., Fan, F., Bai, P., and Liu, J. (2019). Discrete element method simulation on the immigration of granular matter in a vertically vibrating U-tube. J Univ Shanghai Sci Technol 41, 409–416.

Hansen, M., Lanes, G.C., Brito, V.L.G., and Leonel, E.D. (2021). Investigation of pollen release by poricidal anthers using mathematical billiards. Phys Rev E 104, 034409.

Heinrich, B. (2004). Bumblebee Economics. Cambridge: Harvard University Press.

Huang, S.Q., and Shi, X.Q. (2013). Floral isolation in *Pedicularis*: how do congeners with shared pollinators minimize reproductive interference? New Phytol 199, 858–865.

Jankauski, M., Ferguson, R., Russell, A., and Buchmann, S. (2022). Structural dynamics of real and modelled *Solanum* stamens: implications for pollen ejection by buzzing bees. J R Soc Interface 19, 20220040.

Kemp, J.E., and Vallejo-Marín, M. (2021). Pollen dispensing schedules in buzz-pollinated plants: experimental comparison of species with contrasting floral morphologies. Am J Bot 108, 993–1005.

King, M.J., and Buchmann, S.L. (2003). Floral sonication by bees: Mesosomal vibration by *Bombus* and *Xylocopa*, but not *Apis* (Hymenoptera: Apidae), ejects pollen from poricidal anthers. J Kansas Entom Soc 76, 295–305.

Koch, L., Lunau, K., Wester, P., and Borges, R.M. (2017). To be on the safe site—ungroomed spots on the bee's body and their importance for pollination. PLoS One 12, e0182522.

Latty, T., and Trueblood, J.S. (2020). How do insects choose flowers? A review of

multi-attribute flower choice and decoy effects in flower-visiting insects. J Anim Ecol 89, 2750–2762.
Lautenschleger, A., Vizentin-Bugoni, J., Cavalheiro, L.B., and Iserhard, C.A. (2021). Morphological matching and phenological overlap promote niche partitioning and shape a mutualistic plant-hawkmoth network. Ecol Entomol 46, 292–300.
Liang, H., Ren, Z., Tao, Z., Zhao, Y., Bernhardt, P., Li, D., Wang, H., and Scopece, G. (2018). Impact of pre- and post-pollination barriers on pollen transfer and reproductive isolation among three sympatric *Pedicularis* (Orobanchaceae) species. Plant Biol 20, 662–673.
Liang, H., Zhao, Y.H., Rafferty, N.E., Ren, Z.X., Zhong, L., Li, H.D., Li, D.Z., and Wang, H. (2021). Evolutionary and ecological factors structure a plant-bumblebee network in a biodiversity hotspot, the Himalaya-Hengduan Mountains. Funct Ecol 35, 2523–2535.
Luo, Z., Zhang, D., and Renner, S.S. (2008). Why two kinds of stamens in buzz-pollinated flowers? Experimental support for Darwin's division-of-labour hypothesis. Funct Ecol 22, 794–800.
Macior, L.W. (1983). The pollination dynamics of sympatric species of *Pedicularis* (Scrophulariaceae). Am J Bot 70, 844–853.
Macior, L.W., and Sood, S.K. (1991). Pollination ecology of *Pedicularis megalantha* D. Don (Scrophulariaceae) in the Himachal Himalaya. Plant Spec Biol 6, 75–81.
Macior, L.W., Ya, T., and Zhang, J. (2001). Reproductive biology of *Pedicularis* (Scrophulariaceae) in the Sichuan Himalaya. Plant Spec Biol 16, 83–89.
McKee, C.T., Last, J.A., Russell, P., and Murphy, C.J. (2011). Indentation versus tensile measurements of Young's modulus for soft biological tissues. Tissue Eng Part B-Rev 17, 155–164.
Nevard, L., Russell, A.L., Foord, K., and Vallejo-Marín, M. (2021). Transmission of bee-like vibrations in buzz-pollinated plants with different stamen architectures. Sci Rep 11, 13541.
Peat, J., Tucker, J., and Goulson, D. (2005). Does intraspecific size variation in bumblebees allow colonies to efficiently exploit different flowers? Ecol Entomol 30, 176–181.
Peralta, G., CaraDonna, P.J., Rakosy, D., Fründ, J., Pascual Tudanca, M.P., Dormann, C.F., Burkle, L.A., Kaiser-Bunbury, C.N., Knight, T.M., Resasco, J., et al. (2024). Predicting plant-pollinator interactions: concepts, methods, and challenges. Trends Ecol Evol 39, 494–505.
Peralta, G., Vázquez, D.P., Chacoff, N.P., Lomáscolo, S.B., Perry, G.L.W., Tylianakis, J. M., and Irwin, R. (2020). Trait matching and phenological overlap increase the spatio-temporal stability and functionality of plant-pollinator interactions. Ecol Lett 23, 1107–1116.
Pritchard, D.J., and Vallejo-Marín, M. (2020). Floral vibrations by buzz-pollinating bees achieve higher frequency, velocity and acceleration than flight and defence vibrations. J Exp Biol 223, jeb.220541.
Raine, N.E., and Chittka, L. (2007). Pollen foraging: learning a complex motor skill by bumblebees (*Bombus terrestris*). Naturwissenschaften 94, 459–464.
Reith, M., Classen-Bockhoff, R., and Speck, T. (2004). Biomechanics of salvia flowers: the role of lever and flower tube in specialization on pollinators. In: Symposium on Ecology and Biomechanics Held at the Annual Meeting of the Society-for-Experimental-Biology. Edinburgh: CRC Press-Taylor & Francis Group.
Richmond, B.G., Wright, B.W., Grosse, I., Dechow, P.C., Ross, C.F., Spencer, M.A., and Strait, D.S. (2005). Finite element analysis in functional morphology. Anat Rec 283A, 259–274.
Rosi-Denadai, C.A., Araújo, P.C.S., Campos, L.A.O., Cosme Jr., L., and Guedes, R.N.C. (2020). Buzz-pollination in Neotropical bees: genus-dependent frequencies and lack of optimal frequency for pollen release. Insect Sci 27, 133–142.
Russell, A.L., Golden, R.E., Leonard, A.S., and Papaj, D.R. (2016). Bees learn preferences for plant species that offer only pollen as a reward. Behav Ecol 27, 731–740.
Sánchez, I., Darias, J.R., Paredes, R., Lobb, C.J., and Gutiérrez, G. (2009). Vertical granular transport in a vibrated U-tube. In: Appert-Rolland, C., Chevoir, F., Gondret, P., Lassarre, S., Lebacque, J.P., and Schreckenberg, M., eds. Traffic and Granular Flow '07. Springer, Berlin: Heidelberg. 545–554.
Shirmohammadi, M., Shirmohammadi, M., Yarlagadda, P., Shirmohammadi, M., and Yarlagadda, P. (2017). Determining of Poisson's ratio and Young's modulus of pumpkin tissue—using laser measurement sensors. In: International Conference on Materials Manufacturing and Modelling (ICMMM). Vellore.
Stang, M., Klinkhamer, P.G.L., Waser, N.M., Stang, I., and van der Meijden, E. (2009). Size-specific interaction patterns and size matching in a plant-pollinator interaction web. Ann Bot 103, 1459–1469.
Switzer, C.M., Hogendoorn, K., Ravi, S., and Combes, S.A. (2016). Shakers and head bangers: differences in sonication behavior between Australian *Amegilla murrayensis* (blue-banded bees) and North American *Bombus impatiens* (bumblebees). Arthropod-Plant Interact 10, 1–8.
ter Braak, C.J.F., Cormont, A., and Dray, S. (2012). Improved testing of species traits-environment relationships in the fourth-corner problem. Ecology 93, 1525–1526.
Thorp, R.W. (2000). The collection of pollen by bees. Plant Syst Evol 222, 211–223.
Tong, Z.Y., and Huang, S.Q. (2016). Pre- and post-pollination interaction between six co-flowering *Pedicularis* species via heterospecific pollen transfer. New Phytol 211, 1452–1461.
Vallejo-Marín, M. (2019). Buzz pollination: studying bee vibrations on flowers. New Phytol 224, 1068–1074.
Vallejo-Marín, M., Pereira Nunes, C.E., and Russell, A.L. (2022). Anther cones increase pollen release in buzz-pollinated *Solanum* flowers. Evolution 76, 931–945.
Vallejo-Marín, M., and Russell, A.L. (2024). Harvesting pollen with vibrations: towards an integrative understanding of the proximate and ultimate reasons for buzz pollination. Ann Bot 133, 379–398.
van der Kooi, C.J., Vallejo-Marín, M., and Leonhardt, S.D. (2021). Mutualisms and (A) symmetry in plant-pollinator interactions. Curr Biol 31, R91–R99.
Wang, H., and Li, D.Z. (2005). Pollination biology of four *Pedicularis* species (Scrophulariaceae) in northwestern Yunnan, China. Ann Mo Bot Gard 92, 127–138.
Westerkamp, C. (1997). Keel blossoms: bee flowers with adaptations against bees. Flora 192, 125–132.
Whitney, H.M., and Federle, W. (2013). Biomechanics of plant–insect interactions. Curr Opin Plant Biol 16, 105–111.
Williams, P.H. (2022). The bumblebees of the Himalaya. AbcTaxa 21.
Woodrow, C., Jafferis, N., Kang, Y., and Vallejo-Marín, M. (2024). Buzz-pollinating bees deliver thoracic vibrations to flowers through periodic biting. Curr Biol 34, 4104–4113.e3.
Wu, Z.Y., Li, X.W., and Editorial Committee of Flora Yunnanica. (2006). Flora Yunnanica (Vol. 16). Beijing: Science Press.
Yu, W.B., Liu, M.L., Wang, H., Mill, R.R., Ree, R.H., Yang, J.B., and Li, D.Z. (2015). Towards a comprehensive phylogeny of the large temperate genus *Pedicularis* (Orobanchaceae), with an emphasis on species from the Himalaya-Hengduan Mountains. BMC Plant Biol 15, 176.